
MITU-NET: A FINE-TUNED U-NET WITH SEGFORMER BACKBONE FOR SEGMENTING PUBIC SYMPHYSIS-FETAL HEAD

A PREPRINT

• **Fangyijie Wang**
School of Medicine
University College Dublin
fangyijie.wang@ucdconnect.ie

Guénolé Silvestre
School of Computer Science
University College Dublin
guenole.silvestre@ucd.ie

• **Kathleen Curran**
School of Medicine
University College Dublin
kathleen.curran@ucd.ie

ABSTRACT

Ultrasound measurements have been examined as potential tools for predicting the likelihood of successful vaginal delivery. The angle of progression (AoP) is a measurable parameter that can be obtained during the initial stage of labor. The AoP is defined as the angle between a straight line along the longitudinal axis of the pubic symphysis (PS) and a line from the inferior edge of the PS to the leading edge of the fetal head (FH). However, the process of measuring AoP on ultrasound images is time consuming and prone to errors. To address this challenge, we propose the Mix Transformer U-Net (MiTU-Net) network, for automatic fetal head-pubic symphysis segmentation and AoP measurement. The MiTU-Net model is based on an encoder-decoder framework, utilizing a pre-trained efficient transformer to enhance feature representation. Within the efficient transformer encoder, the model significantly reduces the trainable parameters of the encoder-decoder model. The effectiveness of the proposed method is demonstrated through experiments conducted on a recent transperineal ultrasound dataset. Our model achieves competitive performance, ranking 5th compared to existing approaches. The MiTU-Net presents an efficient method for automatic segmentation and AoP measurement, reducing errors and assisting sonographers in clinical practice. Reproducibility: Framework implementation and models available on <https://github.com/13204942/MiTU-Net>.

Keywords Fetal Ultrasound · Fine-tuning · Transformer · Semantic Segmentation

1 Introduction

Assessing the progression of labor is vital to ensure proper advancement in peripartum care. This assessment enables early detection of any deviations from the expected course, aiming to minimize potential complications for both the mother and fetus. The International Society of Ultrasound in Obstetrics and Gynecology (ISUOG) recommends the implementation of ultrasound biometric technology, particularly the angle of progression (AoP), when assessing the fetal craniopubic symphysis structure Ghi et al. [2018], shown in Figure 1. Thus, the measurement of AoP proves to be a superior method for assessing labor progression. AOP is defined as the angle between a straight line extending along the longitudinal axis of the pubic symphysis (PS) and a line connecting the inferior edge of the PS to the leading edge of the fetal head (FH) Lu et al. [2022a]. The current measurement of AoP is manual assessments conducted by experienced physicians. However, this process is time-consuming, cumbersome, and prone to measurement errors. To address this problem, an algorithm for the automatic measurement of AoP is highly demand in clinical practice. This contribution improves the accuracy of labor progress assessment. The accurate segmentation of the FH and PS regions from ultrasound images is an essential prerequisite for the automated measurement of AoP.

In recent years, deep learning (DL) technology experienced significant advancements. In the field of medical imaging analysis, convolutional neural networks (CNNs), a type of deep learning technology, have demonstrated impressive performance in a wide range of medical imaging applications. Three notable architectures are fully convolutional networks (FCNs) Long et al. [2015], U-Net Ronneberger et al. [2015], and the three-dimensional V-Net Milletari et al. [2016]. These architectures have gained recognition as classic models for analyzing medical images.

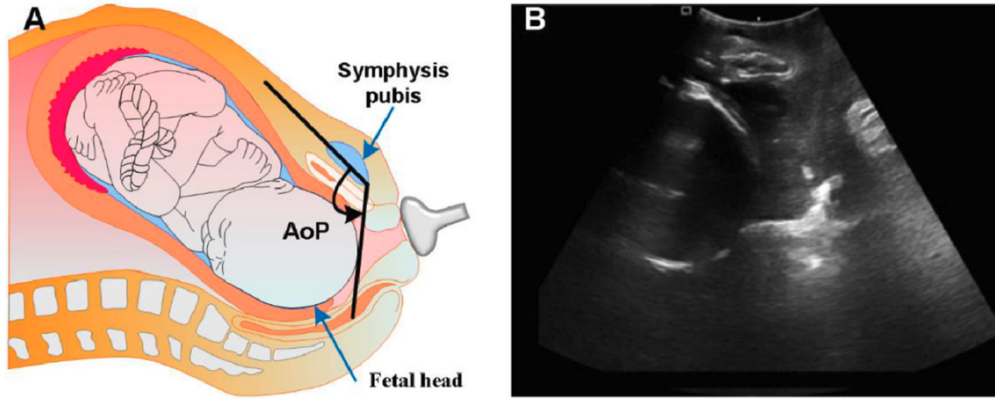


Figure 1: The illustration of the process of measuring the angle of progression (AoP) using transperineal ultrasound. (A) Schematic diagram of calculating AoP. (B) An image showing the symphysis pubis and fetal head.

Recently, researchers have made attempts to combine CNN and Transformer Vaswani et al. [2017b] architectures for the purpose of medical image segmentation. Chen et al. [2021] propose to combine U-Net and Transformer to obtain TransUnet for medical image segmentation. To analysis pregnancy ultrasound images with automatic DL algorithms, Chen et al. [2024] propose a model incorporating a dual attention module, a multi-scale feature screening module and a direction guidance block for segmenting the fetal head and pubic symphysis. This model offers significant advantages in extracting global contextual information and refining segmentation results with direction guidance.

This paper introduces an efficient segmentation network based on the encoder-decoder framework, U-Net, for the automated segmentation of ultrasound images and the measurement of AoP. We enhance the U-Net architecture by replacing its encoder path with a pre-trained Mix Transformer Xie et al. [2021]. The Mix Transformer encoder includes attention mechanisms to enhance feature representation. Furthermore, it reduces computational cost and memory usage by selecting and processing only important parts of the input. Additionally, it significantly reduces the number of trainable parameters from 31 million to 5 million in comparison to the traditional U-Net.

The rest of this paper is organized as follows. Section 2 presents the detailed description of the proposed model. Section 3 focuses on the analysis and evaluation of the experimental results.

2 Methodology

This section introduces an efficient and powerful segmentation fine-tuned model with low computationally demanding modules, MiTU-Net, see Figure 2. The model consists of a U-Net architecture with a pre-trained Mix Transformer encoder for segmenting pubic symphysis-fetal head on a ultrasound dataset, JNU-IFM Lu et al. [2022b]. The U-Net architecture is followed the design from Ronneberger Ronneberger et al. [2015] in 2015. The contracting path ("encoder") of the U-Net is replaced with a pre-trained Mix Transformer encoder (MiT-B0) designed by Xie in SegFormer framework Xie et al. [2021] in 2021. The framework is developed by programming language Python, library PyTorch, and library Segmentation Models Iakubovskii [2019].

2.1 Model Achitecture

Our U-Net architecture contains the contracting path ("encoder") and the expansive path ("decoder"). They both have the same depth of four layers. Between encoder and decoder, we use skip connections to concatenating features from the Mix Transformer encoder to recover spatial information lost during downsampling. We first transpose the original ultrasound image of size $3 \times 256 \times 256$ to size of $256 \times 256 \times 3$. Then the Mix Transformer encoder divides the ultrasound image into small patches of size 4×4 . These patches are the input to the Mix Transformer encoder to obtain multi-level features at $\{1/4, 1/8, 1/16, 1/32\}$ of the original image resolution. The encoder passes the multi-level features to the decoder to predict the segmentation mask at a $\frac{H}{4} \times \frac{W}{4} \times N_{cls}$ resolution, where N_{cls} is the number of categories. The JNU-IFM dataset contains three categories labeled as 0, 1, or 2, with 0 representing the background, 1 representing the pubic symphysis, and 2 representing the fetal head.

Feature Representation The Mix Transformer encoder is a hierarchical type of Transformer encoder that produces multi-level features. It provides both high-resolution coarse features and low-resolution fine features. Specifically, the

encoder creates a hierarchical feature map consisting of a resolution of $\frac{H}{2^{i+1}} \times \frac{W}{2^{i+1}} \times C_i$, where $i \in \{1, 2, 3, 4\}$, by merging multiple patches extracted from the input ultrasound image.

Overlapped Patch Merging We reproduce the Overlapped Patch Merging (OPM) process proposed by Xie et al. [2021] in the patch merging process for SegFormer. It requires K , S , and P , where K is the patch size, S is the stride between two adjacent patches, and P is the padding size. In the first OPM step, we set $K = 7$, $S = 4$, $P = 3$, and $K = 3$, $S = 2$, $P = 1$ for the rest of OPM steps to perform patch merging to produce features.

Self-Attention We apply the multi-head self-attention process Vaswani et al. [2017a], each of the heads Q, K, V have the same dimensions $H \times W \times C$, where H is the height of input image, W is the width of input image, and C is the number of channels. The self-attention is estimated as:

$$\text{Attention}(Q, K, V) = \text{Softmax}\left(\frac{QK^\top}{\sqrt{d_{\text{head}}}}\right)V \quad (1)$$

The computational complexity of this process is $O(N^2)$,

Feed-forward Network We use a feed-forward network (FFN) after the self-attention module. This FFN contains a 3×3 depth-wise convolution that can provide positional information for Transformers sufficiently and reduce computational cost Xie et al. [2021]. It is formulated as follows:

$$\begin{aligned} \hat{\mathbf{x}}_{out} &= \text{Linear}(C_{in}, C_{out})(\mathbf{x}_{in}) \\ \mathbf{x}_{out} &= \text{Linear}(C_{out}, C_{in})(\text{GELU}(\text{DWConv}_{3 \times 3}(\hat{\mathbf{x}}_{out}))) \end{aligned} \quad (2)$$

where \mathbf{x}_{in} is the feature map from the self-attention module, and $\text{Linear}(C_{in}, C_{out})(\cdot)$ is a linear layer with C_{in} and C_{out} as input and output vector dimensions respectively. $\text{DWConv}_{3 \times 3}$ refers to the 3×3 depth-wise convolution.

2.2 Decoder

The decoder path is symmetric to the encoder path. In total it has four convolutional layers. Every layer consists of an upsampling of the feature map followed by a 2×2 up-convolution that halves the number of feature channels, a concatenation with the correspondingly cropped feature map from the encoder path, and two 3×3 convolutions, each followed by a ReLU. The bottom of decoder path is a single 3×3 ("segmentation head") up-convolution followed by a Softmax that outputs a segmentation map with 3 channels. We formulate the decoder's single layer as:

$$\begin{aligned} \hat{X}_{out} &= \text{Conv}_{3 \times 3}(C_F, C_{out})(F) \\ \hat{X}_{out} &= \text{ReLU}(\text{BatchNorm2d}(\hat{X}_{out})) \\ X_{out} &= \text{Conv}_{3 \times 3}(C_{out}, C_{out})(\hat{X}_{out}) \\ X_{out} &= \text{ReLU}(\text{BatchNorm2d}(X_{out})) \end{aligned} \quad (3)$$

where F refers to the feature maps from Mix Transformer encoder path concatenated with the upsampling feature maps from decoder path, C_F refers to the dimensions of the concatenated feature maps F , and C_{out} is the output vector dimensions.

2.3 Data pre-processing and augmentation

The JNU-IFM dataset has 4000 ultrasound images in total. All of them are used for training. We randomly select 30 ultrasound images for validation during training. The size of images is $3 \times 256 \times 256$. We apply one hot encoding on ground truth masks for semantic segmentation, accordingly the ground truth prediction has 3 channels, background prediction, pubic symphysis prediction, and fetal head prediction.

Initially, we are inspired by the regularization technique of randomly masking out square regions of input during training DeVries and Taylor [2017], therefore, we randomly mask out 4×4 square regions of the input images. The number of masked regions is in range $[0, 4]$. Additionally, we pick a random angle from $[-25^\circ, 25^\circ]$ to rotate the input image. Also, we randomly flip the input image horizontally with 50% probability, and vertically with 30% probability. All of input pixels are normalized with mean values $[0.0, 0.0, 0.0]$, and standard deviation values $[1.0, 1.0, 1.0]$. The validation images have no augmentation, but their input pixels are also normalized with mean values $[0.0, 0.0, 0.0]$, and standard deviation values $[1.0, 1.0, 1.0]$.

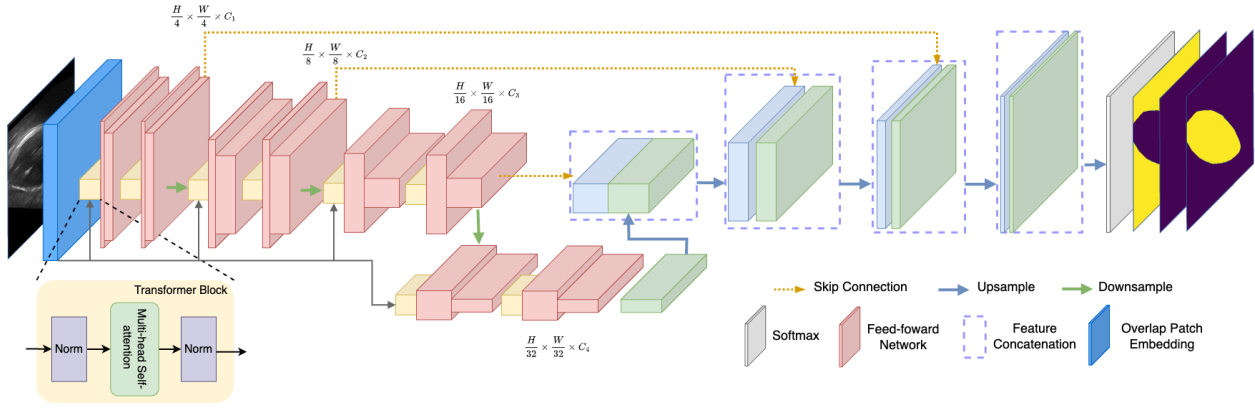


Figure 2: The illustration of the proposed MiTU-Net for automatic fetal head (FH)-pubic symphysis (PS) segmentation.

2.4 Fine-tuning

We implemented all of our experiments using PyTorch, then we trained the entire U-Net with pre-trained MiT-B0 encoder with 20 epochs from scratch. The training dataset and validation dataset both have a batch size of 10. The Adam optimiser was used in training processes with a learning rate of $1e-4$. All training processes were performed on an NVIDIA Tesla T4 graphics card.

Loss Function During the training process, we construct the loss function for this segmentation task with the Binary Cross Entropy loss function and Jaccard Index. Given a predicted mask \hat{Y} and a ground truth mask Y , the loss function can be formulated as follows:

$$\mathcal{L} = \text{BCE}(Y, \hat{Y}) + (1 - \text{J}(Y, \hat{Y})) \quad (4)$$

where BCE refers to the Binary Cross Entropy loss function, and J refers to the Jaccard Index (or Intersection over Union).

Evaluation Metrics The typical metrics applied to evaluate the performance of this U-Net architecture are Pixel Accuracy (PA), Dice coefficient Dice [1945], and Mean Intersection over Union (IoU) Jaccard [1912]. Mean IoU is defined as the average IoU over all classes K . These metrics can be computed using true positive (TP), false positive (FP), true negative (TN) and false negative (FN) of the segmentation results Tavakoli et al. [2021]. TP represents the pixels considered as being in the object and being really in the object, conversely, TN is the pixels outside the object both in the segmentation and the ground truth. FP represents the pixels considered by the segmentation in the object, but which in reality are not part of it. Finally, FN represents the pixels of the object that the segmentation has classified outside.

3 Experiments Results

3.1 Evaluation Metrics

The typical metrics applied to evaluate the performance of segmentation models are Dice similarity coefficient (DSC) Dice [1945], Hausdorff Distance (HD) Birsan and Tiba [2006], Average Surface Distance (ASD) Yeghiazaryan and Voiculescu [2018], and the AoP difference (ΔAoP) between predicted and manually measured AoP for prediction. The DSC is employed to assess the level of similarity between a predicted segmentation mask and the ground truth segmentation mask. The DSC values range from 0, representing no overlap, to 1, indicating perfect overlap. HD measures the maximum spatial dissimilarity between corresponding points in the predicted and ground truth masks. On the other hand, the ASD quantifies the average spatial dissimilarity between the predicted and ground truth masks, offering a different perspective on segmentation accuracy. The final evaluation metrics can be defined by 5:

$$\begin{aligned}
S = & 0.25 \left(\frac{DSC_{FH} + DSC_{PS} + DSC_{ALL}}{3.0} \right) \\
& + 0.25 \left[\frac{0.5 \left(1 - \frac{HD_{FH}}{100} + 1 - \frac{HD_{PS}}{100} + 1 - \frac{HD_{ALL}}{100} \right)}{3.0} + \frac{0.5 \left(1 - \frac{ASD_{FH}}{100} + 1 - \frac{ASD_{PS}}{100} + 1 - \frac{ASD_{ALL}}{100} \right)}{3.0} \right] \\
& + 0.5 \left(1 - \frac{\Delta AoP}{180} \right)
\end{aligned} \tag{5}$$

Besides, the visualization of the segmentation results obtained by MiTU-Net is shown in Figure 3. The second row displays the ground truth masks, while the third row presents the segmentation details obtained from MiTU-Net. The results indicate a competitive performance of MiTU-Net in segmenting the pubic symphysis and fetal head shapes.

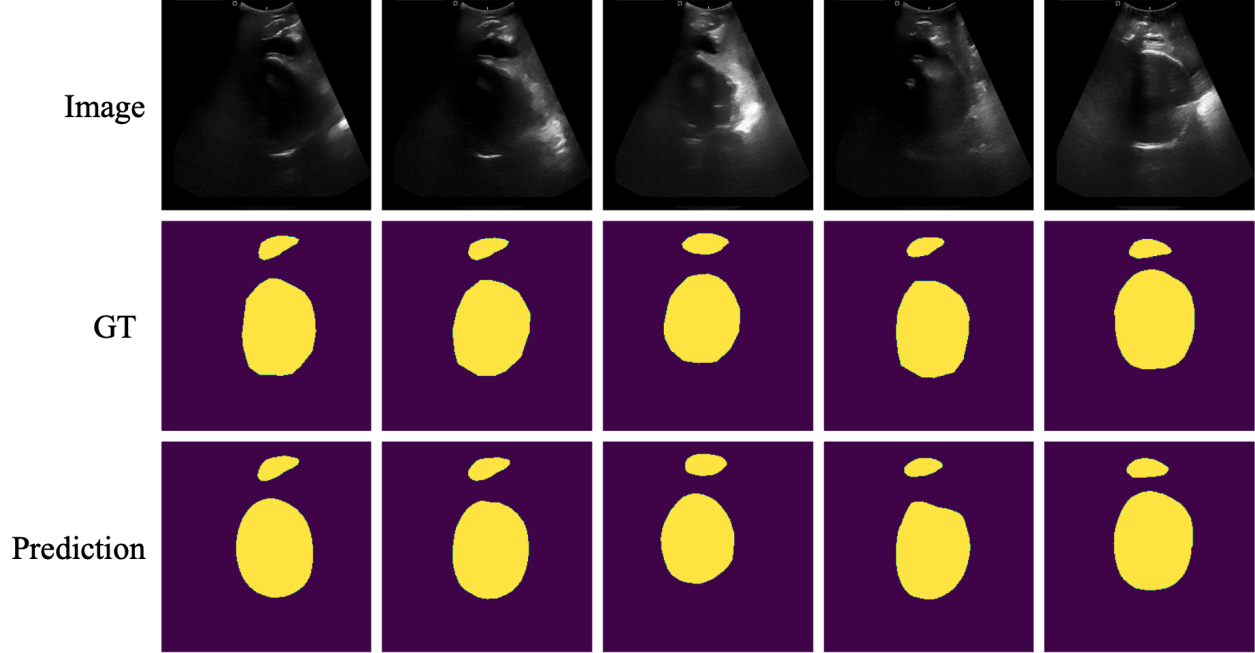


Figure 3: Visualization of segmentation results on the JNU-IFM dataset. GT: Ground Truth

3.2 Compare with SOTA Methods

Compared to other methods, our proposed method achieved the 5th place in the FH-PS-AOP challenge, shown in Table 1. The MiTU-Net achieves a final score of 0.9283, demonstrating its effectiveness. Moreover, its average Dice score of 0.9247 for the fetal head and public symphysis demonstrates its competitiveness, surpassing even the rank 1 method. However, it is noteworthy that our method has big gap between top-ranking methods on HD for fetal head and pubic symphysis. We believe the reason for this is that HD is not considered as a loss during fine-tuning process.

Acknowledgments

This publication has emanated from research conducted with the financial support of Science Foundation Ireland under Grant number 18/CRT/6183. For the purpose of Open Access, the author has applied a CC BY public copyright licence to any Author Accepted Manuscript version arising from this submission.

References

T. Birsan and D. Tiba. One hundred years since the introduction of the set distance by dimitrie pompeiu. In *System Modeling and Optimization*, pages 35–39. Springer US, 2006.

Table 1: The final segmentation results of top 7 methods evaluated on the FH-PS-AOP dataset.

Rank	Author	Final Score	AOP	HD FH	HD PS	HD All	ASD FH	ASD PS	ASD All	Dice FH	Dice PS	Dice All
1	Stock	0.9418	6.5437	12.6313	7.6385	13.4477	3.8963	2.4086	3.4857	0.9303	0.8833	0.9236
2	Elbatel	0.9416	7.9698	10.6985	7.5586	12.0595	3.3069	2.9945	2.9811	0.9403	0.8881	0.9346
3	Qiu	0.9388	7.6472	12.4586	7.6612	13.6147	3.6155	2.2572	3.2383	0.9358	0.8696	0.9295
4	Chen	0.9312	8.5581	14.0105	9.0512	15.3342	3.8692	2.6199	3.5173	0.9314	0.8596	0.9240
5	Ours	0.9283	8.7188	14.0093	10.8286	15.8089	3.9837	2.9824	3.5785	0.9313	0.8580	0.9247
6	Sun	0.9230	9.2760	15.7951	11.5361	17.5598	4.7231	3.1139	4.2646	0.9179	0.8370	0.9096
7	Cai	0.8974	12.1990	20.0307	14.0684	21.8731	7.0988	4.2081	6.0576	0.8787	0.8036	0.8725

- J. Chen, Y. Lu, Q. Yu, X. Luo, E. Adeli, Y. Wang, L. Lu, A. L. Yuille, and Y. Zhou. Transunet: Transformers make strong encoders for medical image segmentation. *arXiv*, 2021.
- Z. Chen, Z. Ou, Y. Lu, and J. Bai. Direction-guided and multi-scale feature screening for fetal head–pubic symphysis segmentation and angle of progression calculation. *Expert Systems with Applications*, 245:123096, July 2024.
- T. DeVries and G. W. Taylor. Improved regularization of convolutional neural networks with cutout, 2017.
- L. R. Dice. Measures of the amount of ecologic association between species. *Ecology*, 26(3):297–302, July 1945.
- T. Ghi, T. Eggebø, C. Lees, K. Kalache, P. Rozenberg, A. Youssef, L. J. Salomon, and B. Tutschek. ISUOG practice guidelines: intrapartum ultrasound. *Ultrasound Obstet. Gynecol.*, 52(1):128–139, July 2018.
- P. Iakubovskii. Segmentation models pytorch. https://github.com/qubvel/segmentation_models.pytorch, 2019.
- P. Jaccard. The distribution of the flora in the alpine zone. *New Phytol.*, 11(2):37–50, Feb. 1912.
- J. Long, E. Shelhamer, and T. Darrell. Fully convolutional networks for semantic segmentation. In *Proceedings of the IEEE Conference on Computer Vision and Pattern Recognition (CVPR)*, June 2015.
- Y. Lu, M. Zhou, D. Zhi, M. Zhou, X. Jiang, R. Qiu, Z. Ou, H. Wang, D. Qiu, M. Zhong, X. Lu, G. Chen, and J. Bai. The JNU-IFM dataset for segmenting pubic symphysis-fetal head. *Data Brief*, 41(107904):107904, Apr. 2022a.
- Y. Lu, M. Zhou, D. Zhi, M. Zhou, X. Jiang, R. Qiu, Z. Ou, H. Wang, D. Qiu, M. Zhong, X. Lu, G. Chen, and J. Bai. The JNU-IFM dataset for segmenting pubic symphysis-fetal head. *Data in Brief*, 41:107904, 2022b. ISSN 2352-3409. doi:<https://doi.org/10.1016/j.dib.2022.107904>. URL <https://www.sciencedirect.com/science/article/pii/S2352340922001160>.
- F. Milletari, N. Navab, and S.-A. Ahmadi. V-net: Fully convolutional neural networks for volumetric medical image segmentation. In *2016 Fourth International Conference on 3D Vision (3DV)*, pages 565–571, 2016. doi:10.1109/3DV.2016.79.
- O. Ronneberger, P. Fischer, and T. Brox. U-Net: Convolutional networks for biomedical image segmentation. In *LNCS: Medical Image Computing and Computer-Assisted Intervention (MICCAI)*, volume 9351, pages 234–241. Springer, 2015. ISBN 978-3-319-24574-4.
- S. Tavakoli, A. Ghaffari, Z. M. Kouzehkhanan, and R. Hosseini. New segmentation and feature extraction algorithm for classification of white blood cells in peripheral smear images. *Sci. Rep.*, 11(1):19428, Sept. 2021.
- A. Vaswani, N. Shazeer, N. Parmar, J. Uszkoreit, L. Jones, A. N. Gomez, L. Kaiser, and I. Polosukhin. Attention is all you need. In I. Guyon, U. von Luxburg, S. Bengio, H. M. Wallach, R. Fergus, S. V. N. Vishwanathan, and R. Garnett, editors, *Advances in Neural Information Processing Systems 30: Annual Conference on Neural Information Processing Systems 2017, December 4-9, 2017, Long Beach, CA, USA*, pages 5998–6008, 2017a. URL <https://proceedings.neurips.cc/paper/2017/hash/3f5ee243547dee91fbd053c1c4a845aa-Abstract.html>.
- A. Vaswani, N. Shazeer, N. Parmar, J. Uszkoreit, L. Jones, A. N. Gomez, L. u. Kaiser, and I. Polosukhin. Attention is all you need. In I. Guyon, U. V. Luxburg, S. Bengio, H. Wallach, R. Fergus, S. Vishwanathan, and R. Garnett, editors, *Advances in Neural Information Processing Systems*, volume 30. Curran Associates, Inc., 2017b. URL https://proceedings.neurips.cc/paper_files/paper/2017/file/3f5ee243547dee91fbd053c1c4a845aa-Paper.pdf.
- E. Xie, W. Wang, Z. Yu, A. Anandkumar, J. M. Alvarez, and P. Luo. Segformer: Simple and efficient design for semantic segmentation with transformers. In *Neural Information Processing Systems (NeurIPS)*, 2021.

V. Yeghiazaryan and I. Voiculescu. Family of boundary overlap metrics for the evaluation of medical image segmentation. *J Med Imaging (Bellingham)*, 5(1):015006, Feb. 2018.